

# **Adaptive Spacecraft Attitude Control With Application to Space Station**

D. Boussalis, D.S. Bayard and S.J. Wang  
Jet Propulsion Laboratory, California Institute of Technology  
4800 Oak Grove Drive, Pasadena, CA 91109

## **Abstract**

Keywords: Adaptive control, attitude control, space station, mobile payload

The attitude control problem of earth orbiting platforms is considered. A model reference adaptive control law has been developed that stably maintains spacecraft attitude at the torque equilibrium under the influence of large mass variations and external disturbances. The result is demonstrated through simulation using the nonlinear dynamic model of the Space Station Freedom.

## **1 Introduction**

Future space missions envision the use of large earth orbiting platforms such as the space station, various space telescopes, interferometers, and planetary exploration spacecraft. Considering that vehicles of large size must be assembled in space, knowledge of their mass and dynamic properties will involve significant uncertainties. This results from the fact that ground structural tests can only be performed on the isolated component and subsystem levels, and in the 1-g environment. Consequently, one should anticipate that in-flight dynamic behavior will deviate significantly from that predicted by analytical models. System parameter uncertainties combined with the effect of on orbit dynamic disturbances such as aerodynamic and gravitational forces, torques generated by astronaut motion in manned vehicles, and transportation of large mobile payloads, introduce significant complexity to the attitude control and vibration suppression problem. Utilization of conventional control techniques will no longer be adequate to ensure stability and meet performance requirements.

The adverse effect of environmental disturbances is particularly apparent in some of the proposed space station configurations, where aerodynamic forces tend to destabilize the vehicle. The attitude control and momentum management problem for this case has been addressed in [1]- [2] under the assumption of well known vehicle dynamics. Stability, however, cannot be guaranteed if there is insufficient knowledge of mass properties, or substantial mass variations, such as those induced by large payload motion.

For systems with significant model uncertainties, one can address the control design problem in two ways: either perform periodical on-orbit parameter identification followed by a fixed gain control design and tuning, or develop a direct adaptive scheme that will continuously adjust control gains to compensate for parameter uncertainties and time-varying plant and environmental effects to ensure stable and robust performance. The former method, that includes indirect adaptive control, has been investigated in [3]- [4]. A potential disadvantage of indirect methods is that they require persistent excitation condition which may not be satisfied under nominal spacecraft motion. In contrast, the present paper considers the design of a direct adaptive controller. This scheme is stable, does not require persistent excitation, and provides the capability to handle sudden or continuous changes in system dynamics, such as those generated by payload motion, vehicle docking, changing configuration, and parameter drift.

The following sections present the derivation of the control law. In Section 2, the nonlinear attitude dynamics of the orbiting spacecraft are discussed and a linearized representation, useful in control design, is derived. In Section 3, model reference adaptive control (MRAC) theory is used to first derive a non adaptive model following control law and then extend it to an adaptive algorithm. A stability proof is given as an integral part of the derivation to show robustness under the effect of large moment of inertia changes and of destabilizing aerodynamic forces. Section 4 gives an application of the algorithm to the 'Phase I' configuration of the Space Station Freedom (SSF) shown in Figure 1.

## 2 Attitude Dynamics and Control

The control problem for space platforms such as the space station is concerned with both attitude stabilization and suppression of flexible body vibrations. These two processes, however, occur at distinctly separated time-scale or frequency bands, thus allowing decoupling of the rigid body from the flexible dynamics. The attitude control loop considered in this paper constitutes an inner (slower) loop in the control system with an effective bandwidth at least one decade below the frequency of the first flexible mode. The resulting control system is adequate to handle the environmental disturbances that, typically, vary at the orbital rate. The control law is generically developed using the linearized attitude dynamics of a rigid spacecraft. Performance evaluation is then conducted via simulation with the nonlinear dynamic model of the SSF.

This paper deals with the attitude control problem only, and assumes that the torque equilibrium angle (TEA) is known. A momentum management loop is currently under development and will be integrated with the attitude control law presented here.

### 2.1 Assumptions and Definitions

The following analysis assumes a rigid spacecraft on a circular orbit. The attitude control system will enforce a local vertical-local horizontal (LVLH) orientation of the vehicle. Two coordinate systems are of interest at present. The rotating orbital frame  $\mathcal{O}(X, Y, Z)$  in the LVLH orientation with the  $+Z$  axis along the local vertical in the nadir direction, the  $+X$  in the direction of flight, and the  $+Y$  axis normal to the orbital plane defined by the vector  $\hat{Z} \times \hat{X}$ . Then the orbital rate vector in  $\mathcal{O}$  coordinates is

$$\Omega = [0 \quad -\omega_0 \quad 0]^T \quad (2.1)$$

where  $\omega_0$  is the orbital rate. A body fixed coordinate system  $\mathcal{B}(x, y, z)$  is defined to nominally

coincide with  $\mathcal{O}$ . Perturbations of  $\mathcal{B}$  relative to  $\mathcal{O}$  define the spacecraft attitude expressed in terms of the three attitude angles  $\theta_x$ ,  $\theta_y$ , and  $\theta_z$ , the roll, *pitch* and *yaw*, respectively. The body rate components about the  $\mathcal{B}$  axes form the vector

$$\omega = [\omega_x \ \omega_y \ \omega_z]^T \quad (2.2)$$

Using the above definitions and assuming a (2-3-1) rotation sequence of the  $\mathcal{B}$  frame from its original alignment with  $\mathcal{O}$ , one obtains the equation for the attitude kinematics

$$\begin{bmatrix} \dot{\theta}_x \\ \dot{\theta}_y - \omega_x \\ \dot{\theta}_z \end{bmatrix} = [A_\theta] \begin{bmatrix} \omega_x \\ \omega_y \\ \omega_z \end{bmatrix} \quad (2.3)$$

$$A_\theta = \frac{1}{\cos \theta_z} \begin{bmatrix} \cos \theta_z - \cos \theta_x \cos \theta_z & \sin \theta_x \sin \theta_z \\ 0 & \cos \theta_x & -\sin \theta_x \\ 0 & \sin \theta_x \cos \theta_z & \cos \theta_x \cos \theta_z \end{bmatrix} \quad (2.4)$$

The three attitude angles are concatenated in the 3-tuple

$$o = [\theta_x \ \theta_y \ 0]^T \quad (2.5)$$

Let  $I$  denote the inertia tensor

$$I = \begin{bmatrix} I_{11} & I_{12} & I_{13} \\ I_{12} & I_{22} & I_{23} \\ I_{13} & I_{23} & I_{33} \end{bmatrix} \quad (2.6)$$

Assuming that the  $\mathcal{B}$  axes are also the principle axes of the structure, then the off-diagonal terms in (2.6) vanish. To distinguish from the inertia tensor, the symbol  $\mathcal{I}$  will represent the identity matrix. Finally, given any three-vector  $v = [v_1 \ v_2 \ v_3]^T$ , the notation  $\hat{v}$  will be used to denote the cross *product* operator

$$\hat{v} = \begin{bmatrix} 0 & -v_3 & v_2 \\ v_3 & 0 & -v_1 \\ -v_2 & v_1 & 0 \end{bmatrix} \quad (2.7)$$

## 2.2 Rigid Spacecraft Dynamics

The motion of a rigid body is governed by the Euler equations

$$\dot{H} + \tilde{\omega}H = T' \quad (2.8)$$

where  $H$  is the angular momentum vector and  $T'$  is the total external torque. Assuming that the control is effected by utilizing a momentum exchange device, e.g. control moment gyro (CMG),  $H$  takes the form

$$H = I\omega + h \quad (2.9)$$

with

$$\dot{h} = -\tilde{\omega}h + u \quad (2.10)$$

where  $h$  is the angular momentum of the CMG and  $u$  is the control input. Upon substitution of (2.9) and (2.10) into (2.8) yields

$$I\dot{\omega} + \tilde{\omega}I\omega = -\mathbf{u} + T' \quad (2.11)$$

## 2.3 Linearized Attitude Dynamics

For control design purposes, (2.11) may be linearized by expanding to the first order about the constant orbital vector  $\Omega$  to obtain

$$\begin{aligned} I\dot{\omega} &= -\tilde{\Omega}I\Omega - \left. \frac{\partial}{\partial \omega} \tilde{\omega}I\omega \right|_{\omega=\Omega} (\omega - \Omega) - u + T' \\ &= W\omega + G_1\theta - u + \tilde{T}' \end{aligned} \quad (2.12)$$

where

$$\tilde{T}' = W\Omega + G_0 + T'_a \quad (2.13)$$

The matrix  $W$  in (2.12) and (2.13) is given by

$$W = \omega_O \begin{bmatrix} I_{13} & 2I_{23} & I_{33} - I_{22} \\ -I_{23} & 0 & I_{12} \\ I_{22} - I_{11} & -2I_{12} & -I_{13} \end{bmatrix} \quad (2.14)$$

and the quantities  $G_0$  and  $G_1$  by

$$G_0 = \omega_O^2 \begin{bmatrix} -2I_{23} \\ 3I_{13} \\ -I_{12} \end{bmatrix}; \quad G_1 = 3\omega_O^2 \begin{bmatrix} I_{33} - I_{22} & I_{12} & 0 \\ I_{12} & I_{33} - I_{11} & 0 \\ -I_{13} & -I_{23} & 0 \end{bmatrix} \quad (2.15)$$

The aerodynamic force  $T_a$  has the form

$$T_a = q_0 + q_1 \sin \omega_O t + q_2 \sin 2\omega_O t \quad (2.16)$$

The attitude kinematics may now be utilized to eliminate  $\omega$  from (2.12). Assuming small angles (2.3) yields

$$\dot{\theta} = \hat{\Omega}\theta + \omega - \Omega \quad \text{and} \quad \ddot{\theta} = \hat{\Omega}\dot{\theta} + \dot{\omega}$$

Then substituting into (2.12) one obtains the linearized description of the attitude dynamics,

$$I\ddot{\theta} - (I\hat{\Omega} + W)\dot{\theta} + (W\hat{\Omega} - G_1)\theta = -u + \bar{T} \quad (2.17)$$

With similar arguments, it can be shown that the CMG angular momentum may be approximately represented by the linear equation

$$\dot{h} = -\hat{\Omega}h + u \quad (2.18)$$

The simplified form of (2.17) will be used in Section 3 to derive the attitude control law.

### 3 Model Reference Attitude Control

The attitude dynamics can be written in the following second-order form,

$$M\ddot{\theta} + D\dot{\theta} + K\theta = B_u u_p + \Gamma_d d \quad (3.1)$$

Equation (3.1) follows from (2.17) with  $M = -I$ ,  $\bar{T} = \Gamma_d d$ ,  $\Gamma_d = [W\hat{\Omega} + G_0 + q_0|q_1|q_2]$ ,  $D = -(I\hat{\Omega} + W)$ ,  $K = W\hat{\Omega} - G_1$ ,  $B_u = I$  and  $u_p = u$ . The bounded disturbance vector  $d$  acting on the spacecraft can be considered solution of the differential equation

$$d = A_d d \quad (3.2)$$

where all the eigenvalues of the matrix  $A_d$  are distinct and lie on the  $j\omega$  axis. Accordingly (see Lemma A2), there is a  $P_d = P_d^T > 0$  such that,

$$P_d A_d + A_d^T P_d = -Q_d = 0 \quad (3.3)$$

It is convenient to put the attitude dynamics (3.1) into state-space form as follows,

$$\begin{aligned} \begin{bmatrix} \dot{\theta} \\ \dot{\varrho} \end{bmatrix} &= \begin{bmatrix} 0 & \mathcal{I} \\ -M^{-1}K & -M^{-1}D \end{bmatrix} \begin{bmatrix} \theta \\ \varrho \end{bmatrix} + \begin{bmatrix} 0 \\ M^{-1}B_u \end{bmatrix} u_p \\ &+ \begin{bmatrix} \theta \\ MM^{-1}\Gamma_d \end{bmatrix} d \end{aligned} \quad (3.4)$$

It is noted that this system has the following general form,

$$\dot{x}_p = A_p x_p + B_p u_p + \Gamma d \quad (3.5)$$

where,

$$x_p = \begin{bmatrix} x_{p1} \\ x_{p2} \end{bmatrix}; \quad A_p = \begin{bmatrix} 0 & \mathcal{I} \\ A_{p1} & A_{p2} \end{bmatrix} \quad (3.6)$$

$$B_p = \begin{bmatrix} 0 \\ B_{p2} \end{bmatrix}; \quad \Gamma = \begin{bmatrix} 0 \\ \Gamma_2 \end{bmatrix} \quad (3.7)$$

By comparison with (3.4) the components of model (3.5) are specified as,  $x_{p1} = \theta$ ,  $x_{p2} = \dot{\theta}$ ,  $A_{p1} = -M^{-1}A'$ ,  $A_{p2} = -M^{-1}D$ ,  $B_{p2} = M^{-1}B_u$ ,  $\Gamma_2 = M^{-1}\Gamma_d$ . Define a reference model of the form,

$$\dot{x}_m = A_m x_m + B_m u_m \quad (3.8)$$

where,

$$A_m = \begin{bmatrix} 0 & \mathcal{I} \\ A_{m1} & A_{m2} \end{bmatrix}; \quad B_m = \begin{bmatrix} 0 \\ B_{m2} \end{bmatrix} \quad (3.9)$$

The reference model can be chosen by the designer to be any stable model of the form (3.8), (3.9). Hence, there exists  $Q = Q^T > 0$  and  $P = P^T > 0$  such that

$$PA_m + A_m^T P = -Q \quad (3.10)$$

### 3.1 Non-Adaptive Control

In this section, a modelreference attitude control law will be designed of the following form,

$$u_p = K^\circ x_p + H^\circ u_m + J^\circ d \quad (3.11)$$

where  $K^\circ, H^\circ$ , and  $J^\circ$  are matrix gains which remain to be chosen. Define a state error vector as,

$$e = x_m - x_p \quad (3.12)$$

The dynamics of  $e$  can be computed as,

$$\begin{aligned} \dot{e} &= A_m x_m + B_m u_m - A_p x_p - B_p u_p - \Gamma d \\ &= A_m e + (A_m - A_p - B_p K^\circ) x_p \\ &\quad + (B_m - B_p H^\circ) u_m - (B_p J^\circ + \Gamma) d \end{aligned} \quad (3.13)$$

The dynamics of  $e$  are simplified by choosing the gains as to the following *Model Reference Attitude Control Law*:

$$\begin{aligned} K^\circ &= [K_1^\circ \ K_2^\circ] \\ K_1^\circ &= B_{p2}^{-1} (A_{m1} - A_{p1}) \\ K_2^\circ &= B_{p2}^{-1} (A_{m2} - A_{p2}) \\ H^\circ &= B_{p2}^{-1} B_{m2} \\ J^\circ &= -B_{p2}^{-1} \Gamma d \end{aligned} \quad (3.14)$$

in which case the error equation (3.13) becomes,

$$\dot{e} = A_m e \quad (3.15)$$

Clearly, using the attitude controller (3.11), (3.14) the error between  $x_p$  and  $x_m$  dies out exponentially according to the dynamics of the reference model  $A_m$ .

**Remark:** If knowledge of  $M, K, D$  is available, the model reference attitude control law can be used for gain scheduling. Since these quantities appear explicitly in the design, i.e., substituting expressions from the second-order model (3.1) gives  $K_1^\circ = M A_{m1} + K$ ;  $K_2^\circ = M A_{m2}$ ;  $H^\circ = M B_{m2}$ ;  $J^\circ = -\Gamma d$ .



### 3.2 Adaptive Control

The nonadaptive attitude control law can be written in vectorized form as,

$$u_p = \Theta^\circ r \quad (3.16)$$

where,

$$\Theta^\circ = [K_1^\circ \ K_2^\circ \ H^\circ \ J^\circ] \quad (3.17)$$

$$r = [x_{p1}^T \ x_{p2}^T \ u_m^T \ d^T]^T \quad (3.18)$$

Suppose that the gain matrix  $\Theta^\circ$  in the control (3.16) is not known, and is replaced by an estimate  $\hat{\Theta}$  to give the approximate control,

$$\hat{u}_p = \hat{\Theta} r \quad (3.19)$$

where,

$$\hat{\Theta} = [\hat{K}_1 \ \hat{K}_2 \ \hat{H} \ \hat{J}] \quad (3.20)$$

In this case, the error dynamics in (3.15) become,

$$\dot{e} = A_m e + B_p \Phi r \quad (3.21)$$

where,

$$\Phi = \Theta^\circ - \hat{\Theta} \quad (3.22)$$

The following partitions will be useful,

$$\Phi = [\Phi_1 \ \Phi_2 \ \Phi_3 \ \Phi_4] \quad (3.23)$$

$$r = [r_1^T \ r_2^T \ r_3^T \ r_4^T]^T \quad (3.24)$$

where comparison with (3.18) gives,  $r_1 = x_{p1}$ ;  $r_2 = x_{p2}$ ;  $r_3 = u_m$ ;  $r_4 = d$  and  $\Phi_1 = K_1^\circ - \hat{K}_1$ ;  $\Phi_2 = K_2^\circ - \hat{K}_2$ ;  $\Phi_3 = H^\circ - \hat{H}$ ;  $\Phi_4 = J^\circ - \hat{J}$ . The partition (3.23-3.24) also leads to the identity,

$$\Phi r = \sum_{i=1}^4 \Phi_i r_i \quad (3.25)$$

A general result for stable tuning of the adaptive attitude controller (3.19) is given next.

**Theorem:** Consider the spacecraft dynamics (3.5) with disturbance model (3.2), reference model (3.8) and tunable attitude control law (3.19). Let the parameters in the attitude controller, be tuned according to the adaptive law,

$$\dot{\Phi}_i = -\Lambda_i S P e r_i^T; \quad i = 1, 2, 3, 4 \quad (3.26)$$

where  $S = [0 | \mathcal{I}]$ , and  $\Lambda_i$  are any matrices such that

$$B_{p2} \Lambda_i^{-1} = (B_{p2} \Lambda_i^{-1})^T > 0 \quad i = 1, 2, 3, 4 \quad (3.27)$$

(e.g.,  $\Lambda_i = \lambda_i \cdot I$ ,  $\lambda_i > 0$ ). Then, the error  $e = x_m - x_p$  in (3.21) approaches zero asymptotically, and the quantities  $x_p, \hat{K}(t), \hat{H}(t)$  and  $\hat{J}(t)$  remain bounded.

**Proof:** Consider the Lyapunov function candidate,

$$V = e^T P e + Tr \left\{ \sum_{i=1}^4 \Phi_i^T B_{p2} \Lambda_i^{-1} \Phi_i \right\} + d^T P_d d \quad (3.28)$$

Differentiating along the system trajectories gives,

$$\begin{aligned} \dot{V} &= e^T P \dot{e} + \dot{e}^T P e + Tr \left\{ \sum_{i=1}^4 \Phi_i^T B_{p2} \Lambda_i^{-1} \dot{\Phi}_i + \dot{\Phi}_i^T B_{p2} \Lambda_i^{-1} \Phi_i \right\} \\ &\quad + d^T P_d \dot{d} + \dot{d}^T P_d d \end{aligned} \quad (3.29)$$

$$\begin{aligned} &= -e^T Q e + 2r^T \Phi^T B_p^T P e + \\ &\quad 2Tr \left\{ \sum_{i=1}^4 \Phi_i^T B_{p2} \Lambda_i^{-1} \dot{\Phi}_i \right\} - d^T Q_d d \end{aligned} \quad (3.30)$$

$$\begin{aligned} &= -e^T Q e + 2 \sum_{i=1}^4 r_i^T \Phi_i^T B_p^T P e \\ &\quad + 2Tr \left\{ \sum_{i=1}^4 \Phi_i^T B_{p2} \Lambda_i^{-1} \dot{\Phi}_i \right\} - d^T Q_d d \end{aligned} \quad (3.31)$$

$$\begin{aligned} &= -e^T Q e + 2Tr \left\{ \sum_{i=1}^4 \Phi_i^T (B_p^T P e r_i^T + B_{p2}^T \Lambda_i^{-1} \dot{\Phi}_i) \right\} \\ &\quad - d^T Q_d d \end{aligned} \quad (3.32)$$

or

$$\dot{V} = -c^T Q c + 2Tr \left\{ \sum_{i=1}^4 \Phi_i^T B_{p2}^T (SPc r_i^T + \Lambda_i^{-1} \dot{\Phi}_i) \right\} - d^T Q_d d \quad (3.33)$$

Here, (3.30) follows from (3.29) by using (3.3), (3.10), (3.27) and properties of the trace; equation (3.31) follows by identity (3.25); equation (3.32) follows by rearranging and using properties of the trace; and (3.33) follows using the definition of S, Then considering (3.3), and substituting adaptive law (3.26) into (3.33) yields,

$$\dot{V} = -c^T Q c < 0 \quad (3.34)$$

This implies that  $V$  and, consequently, the quantities  $c, \Phi, d, x_p, r$  are bounded, Taking an additional derivative of  $V$  gives,

$$\ddot{V} = -2c^T Q \dot{c} = -2c^T Q (A_m c + B_p \Phi r) \quad (3.35)$$

Hence,  $v$  is bounded which implies that  $\dot{V}$  is uniformly continuous. Since,

$$\int_0^\infty \dot{V} dt = V(\infty) - V(0) < \infty \quad (3.36)$$

it follows from Barabalat's lemma [5] that  $V \rightarrow 0$  and hence  $c \rightarrow 0$  as desired.  $\blacksquare$

The adaptive law (3.26) indicates that the feedback gains in the attitude control loop are tuned using the relations:

$$\begin{aligned} \hat{K}_1 &= \Lambda_1 SPc x_{p1}^T \\ \hat{K}_2 &= \Lambda_2 SPc x_{p2}^T \\ \hat{H} &= \Lambda_3 SPc u_m^T \\ \hat{J} &= \Lambda_4 SPc d^T \end{aligned} \quad (3.37)$$

The control system developed in this section is represented by the block diagram of Figure 2.

### 3.3 Discussion

The model reference adaptive controller presented in the preceding section is motivated by an approach for robotic manipulators put forth by Lim and Eslami[6], and has intersection

with other standard full-state SISO-type adaptive designs found, for example, in Landau [7], Astrom and Wittenmark [8], as well as more recent works of Slotine and Li [9], Bayard and Wen [10], and Wen and Kreutz [11]. However, the basic approach of Lim and Eslami has been modified for application to attitude control, including (with the help of Lemma A2) the addition of adaptive filters to reject external disturbance torques acting on the orbiting spacecraft. This approach to adaptive disturbance rejection is similar in spirit to standard methods used in the adaptive filtering literature for noise canceling (cf., Widrow and Stearns [12]). However, adaptive filtering methods are intended for feedforward (open-loop) operation, where there is no stability issue. In contrast, the adaptation of the disturbance filters in the present study is specifically designed to work in concert with the adaptive feedback loop to reject disturbances while ensuring stability of the overall closed-loop system.

#### **4 Application to Space Station**

The result of Section 3 is demonstrated via simulation using the dynamic model of the SSF. The 'Phase I' configuration [13] shown in Figure 2 consists of the fully assembled space station and a massive mobile payload. Payload motion over the seven bay distance effects large moment of inertia changes and center of mass relocation, thus, becoming a major contributor to parameter uncertainty and the cause of instability to conventional controllers. In this particular SSF configuration,  $I_{22} < I_{11} < I_{33}$  so that the open loop attitude dynamics are inherently unstable. Under these operational conditions, adaptive attitude stabilization and control become highly desirable.

The equations of motion discussed in Section 2 hold in this case with some modification to reflect the two-body dynamics occurring with the introduction of the payload. The modified equations are briefly discussed in the following.

## 4.1 Space Station/Mobile Payload Dynamics

Let the  $\mathcal{B}$  reference frame be fixed on the main body with origin  $O_B$  at its center of mass (CM). Then at any instant  $t$ , the position of the moving payload CM relative to  $O_B$ , is specified by the vector  $s(t) = [s_1(t) s_2(t) s_3(t)]^T$ . Consequently the effective moment of inertia becomes time dependent and is given by

$$I(t) = \bar{I} - \beta \hat{s}(t) \hat{s}(t) \quad (4.1)$$

where  $\bar{I} = I_s + I_p$ . Here,  $I_s$  and  $I_p$  are the inertia tensors of the space station and payload, respectively. Furthermore, with  $m_s$  and  $m_p$  masses of the main body and payload, respectively,  $\beta$  is defined by

$$\beta = \frac{m_s m_p}{m_s + m_p} \quad (4.2)$$

The angular momentum for the two-body system is

$$H = (\bar{I} - \beta \hat{s} \hat{s}) \omega + \beta \hat{s} \dot{s} + h \quad (4.3)$$

The equation of motion is then obtained by substituting (4.3) into (2.8)

$$I \dot{\omega} + \hat{\omega} I \omega + f(\omega, s, \dot{s}, \ddot{s}) = -u + T \quad (4.4)$$

when  $I$  is given in (4.1) and  $f$  is defined as,

$$f(\omega, s, \dot{s}, \ddot{s}) = -\beta(\ddot{s} \hat{s} + \dot{s} \dot{\hat{s}}) \omega + \hat{\omega} \hat{s} \dot{s} + \hat{s} \ddot{s} \quad (4.5)$$

Thus, the attitude of the space station is completely characterized by (4.4) and (2.3).

## 4.2 Simulation Results

The adaptive attitude control law (3.26) with the gains implemented according to (3.37) is used to control the of the SSF with its dynamics discussed in the preceding section. The parameter values used in the simulation are summarized in the following table:

Table 1: SSF/Pa load Simulation Parameters

Parameter	Space Station	Payload
Mass (kg)	136080	13608
Inertias ( $\text{kg}\cdot\text{m}^2$ )		
$I_{11}$	3.7096e+07	1.4313e+05
$I_{22}$	7.9681e+06	1.9182e+05
$I_{33}$	4.3212e+07	1.4313e-05
$I_{12}$	-2.8774e+05	0.0
$I_{13}$	-1.1805e+05	0.0
$I_{23}$	1.7707e+05	0.0

The parameter vectors  $q_i$  in the aerodynamic disturbance (2.16) have the values given in Table 2,

Table 2: Aerodynamic Parameters(N-nl)

$q_0$	$q_1$	$q_2$
1.3558e+00	1.3558e+00	6.7791e-01
5.4233e+00	2.7116e+00	6.7791e-01
1.3558e+00	1.3558e+00	6.7791e-01

The orbital rate for the assumed circular orbit is constant,  $\omega_0 = 0.0011$  rad/s. The simulation results shown here represent two possible operational scenarios.

**Case I:** The payload does not maneuver, and remains near the CM of the main body. The commanded attitude is  $\theta_c = [0 \text{ --- } 13,5 \text{ } 0]^T$  where the three angles are in degrees. The roll, pitch and yaw responses are shown in Figures 3-5. The broken lines indicate the trajectories generated by the reference model, Note that the bandwidth of the reference model essentially becomes the effective bandwidth of the nonlinear closed-loop attitude control system. Since the attitude control problem considers only the rigid body dynamics of the space station, reference bandwidth for all three axes is set at 0.00234 rad/s, i.e., approximately one decade below the frequency of the first flexible mode. This low bandwidth assures that there is no interaction between the flexible and attitude dynamics of the spacecraft. Figure 6 shows the angular momentum about the pitch axis. Since the pitch motion converges fast to the commanded TTA, it reaches a non zero average value with the absence of a momentum management loop. When this loop is closed, the steady state momentum will oscillate about

zero. The pitch control torque appears in Figure 7.

**Case H:** The **13,608** kg (30,000 lb) payload travels along the y-axis to a distance of 35 meters, approximately, the length of seven space station bays. The payload motion follows the position profile of Figure 8. Despite the large mass relocation, resulting in moment of inertia changes of, approximately, 30% (Figure 9), the adaptive controller maintains stable attitude control and drives the spacecraft to the commanded orientation. Time response of the three attitude angles is shown in Figures 10-12. Representative gain adaptation trajectories are shown in Figures 13-16. It is noted that, in all cases, the torque demand and angular momentum accumulation are well below the baseline CMG requirement for SSF of J 50 lb-ft and 20,000 lb-ft-s, respectively.

## 5 Summary and Conclusions

An approach to attitude control was introduced based on a direct model reference adaptive control law. Since the physical parameters appear explicitly, the control law can be used either for gain scheduling or for adaptive control. It was shown that the model reference controller can be tuned using an adaptation law derived from Lyapunov's direct method. This led to a globally stable adaptive controller for the attitude control problem. Important features of the approach include stability with respect to arbitrary inertia configurations, and adaptive disturbance rejection filters which tune out periodic torques with frequencies at multiples of the orbital rate.

Simulation results show excellent stability and robustness performance when the spacecraft, in this case the space station, is subjected to significant mass property changes. In Case II of Section 4.2, the adaptive controller maintained stable performance under maneuvering of a massive (30,000 lb) payload from the CM of the main body to a distance of 7 bays (35 m).

A problem closely related to attitude control, is momentum management. Here, one is con-

cerned with the amount of momentum accumulated so that the actuators (CMG's, reaction wheels, etc.) do not saturate. Momentum in the present adaptive scheme can be managed by commanding an indirectly computed estimate of the TFA. A direct adaptive approach to the momentum management problem is presently under study which will provide an outer loop for commanding the reference model input. Other issues such as robustness of the adaptive design to flexible body dynamics, nonidealities, etc., remain to be investigated.

## Acknowledgements

The research described in this paper has been performed at the Jet Propulsion laboratory, California Institute of Technology, under contract with the National Aeronautics and Space Administration.

## Appendix

The following are presented in support of the arguments leading to the Lyapunov equation (3.3) and its utilization in the stability proof of Section 3.2,

**Theorem A1:** If  $A \in \mathcal{R}^{n \times n}$  has distinct eigenvalues, then it is similar to a diagonal matrix.

**Proof:** See [13] ■

**Lemma A1:** Let  $\mathcal{A}_c \in \mathcal{R}^{2 \times 2}$  be in the companion form

$$\mathcal{A}_c = \begin{bmatrix} 0 & 1 \\ -\alpha_0 & -\alpha_1 \end{bmatrix} \quad (\text{A.1})$$

with distinct eigenvalues  $\{\lambda_1, \lambda_2\}$ . Then the similarity transformation

$$A = R^{-1} \mathcal{A}_c R \quad (\text{A.2})$$

with  $R$  the nonsingular Vandermonde matrix,

$$R = \begin{bmatrix} 1 & 1 \\ \lambda_1 & \lambda_2 \end{bmatrix} \quad (\text{A.3})$$



diagonalizes A so that  $A = \text{diag}\{\lambda_1, \lambda_2\}$ .

**Proof:** Follows by substitution of (A.1) and (A.3) into (A.2). ■

**Lemma A2:** Let  $A \in \mathcal{R}^{n \times n}$  be a general matrix with distinct eigenvalues all on the  $j\omega$  axis, Then there exists a  $P = P^T > 0$ ,  $P \in \mathcal{R}^{n \times n}$  such that

$$PA + A^T P = -Q \equiv O \quad (A.4)$$

**Proof:** Since all eigenvalues lie on the  $j\omega$  axis,

$$\lambda(A) = \begin{cases} O, \{\pm j\omega_i\}; & \text{if } n \text{ odd} \\ \{\pm j\omega_i\}; & \text{if } n \text{ even} \end{cases} \quad i = 1, 2, \dots, \bar{n} \quad (A.5)$$

where

$$\bar{n} = \begin{cases} \frac{n}{2} & \text{if } n \text{ even} \\ \frac{n-1}{2} & \text{if } n \text{ odd} \end{cases} \quad (A.6)$$

Taking the case of  $n$  odd to be the most general, assume that  $AC$  is in the block  $2 \times 2$  companion form

$$A_c = \begin{bmatrix} 0 & 0 & 0 & \dots & 0 & 0 \\ 0 & 0 & 1 & \dots & 0 & 0 \\ 0 & -\omega_1^2 & 0 & \dots & 0 & 0 \\ \vdots & \vdots & \vdots & \ddots & \vdots & \vdots \\ 0 & 0 & 0 & \dots & 0 & 1 \\ 0 & 0 & 0 & \dots & -\omega_n^2 & 0 \end{bmatrix} \quad (A.7)$$

and let

$$P_c = \begin{bmatrix} 1 & 0 & 0 & \dots & 0 & 0 \\ 0 & 1 & 0 & \dots & 0 & 0 \\ 0 & 0 & \omega_1^{-2} & \dots & 0 & 0 \\ \vdots & \vdots & \vdots & \ddots & \vdots & \vdots \\ 0 & 0 & 0 & \dots & 1 & 0 \\ 0 & 0 & 0 & \dots & 0 & \omega_n^{-2} \end{bmatrix} \quad (A.8)$$

It is easy then to verify that

$$P_c A_c + A_c^T P_c = 0 \quad (A.9)$$

where  $P_c > 0$ . An identical argument can be made if  $n$  is even by eliminating the first row and column from each of  $A_c$  and  $P_c$ . To further generalize this result let  $A$  be any matrix with distinct eigenvalues  $\lambda(A)$  as in (A.5) and  $n$  odd. According to Theorem A.1 there exists a nonsingular matrix  $T$ , such that

$$T^{-1}AT = A \quad (A.10)$$

Furthermore, by Lemma A.1 a block  $2 \times 2$  Vandermonde matrix  $R$  can be constructed as

$$R = \begin{bmatrix} \mathbf{1} & \mathbf{0} & \mathbf{0} & \dots & \mathbf{0} & \mathbf{0} \\ 0 & 1 & 1 & 1 & \dots & 0 & 0 \\ 0 & j\omega_{11} & -j\omega_1 & \dots & 0 & 0 \\ \vdots & \vdots & \vdots & \ddots & \vdots & \vdots \\ \mathbf{0} & \mathbf{0} & \mathbf{0} & \mathbf{0} & \dots & \mathbf{1} & \mathbf{1} \\ \mathbf{0} & \mathbf{0} & \mathbf{0} & \dots & j\omega_n & -j\omega_n \end{bmatrix} \quad (A.11)$$

so that

$$R^{-1}A_cR = A \quad (A.12)$$

Equating the left-hand side of (A.10) and (A.12) and solving for  $A$  yields

$$A = L^{-1}A_cL \quad (A.13)$$

where  $L = RT^{-1}$ . Then from (A.9) and (A.13) it follows that

$$\begin{aligned} P_c A_c + A_c^T P_c &= 0 \\ \Rightarrow L^T P_c L L^{-1} A_c L + L^T A_c^T (L^{-1})^T L^T P_c L &= 0 \\ \Rightarrow PA + A^T P &= 0 \end{aligned}$$

where  $P = L^T P_c L$ . ■

## References

- [1] Wit, B., K.W. Byun, and V.W. Warren, 'New Approach to Attitude/Momentum Control for the Space Station,' *J. of Guidance, Control and Dynamics*, vol. 12, No. 5, pp. 714-722, 1989.
- [2] Vadali, S., R., and H.-S. Oh, "Space Station Attitude Control and Momentum Management: A Nonlinear Look," *J. of Guidance, Control and Dynamics*, vol. 15, No. 3, pp. 577-586, May-June 1992.
- [3] Elgersma, M.R., G. Stein, M.R. Jackson, and J. Yeichner, "Robust Controller for Space Station Momentum Management," *IEEE Control Systems Magazine*, vol. 12, No. 5, pp. 14-22, October, 1992.
- [4] Bishop, R.H., S.J. Paaynter, and J.W. Sunkel, "Adaptive Control of Space Station with Control Moment Gyros," *IEEE Control Systems Magazine*, vol. 12, No. 5, pp. 23-28, October, 1992.
- [5] Popov, V. M., *Hyperstability of Control Systems*, Springer-Verlag, New York, 1973.
- [6] Lim, K. Y., and M. Eslami, 'Adaptive Controller Designs for Robot Manipulator Systems Using Lyapunov Direct Method,' *IEEE Trans. on Automatic Control*, AC30(12), pp. 1229-1233, 1985.
- [7] Landau, Y.D., *Adaptive Control: The Model Reference Approach*, Marcel Dekker, New York, 1979.
- [8] Astrom, K.J and B. Wittenmark, *Adaptive Control.*, Addison Wesley, New York, 1989.
- [9] Slotine, J.J. and W. Li, "On the Adaptive Control of Robot Manipulators," Proc. ASME Winter Annual Meeting, Anaheim, California, 1986.
- [10] Bayard, D.S. and J.T. Wen, "A New Class of Control Laws for Robotic Manipulators Part II: Adaptive case," *International Journal of Control*, Vol. 47, No. 5, pp. 1387-1406, 1988.
- [11] Wen, J.T. and K. Kreutz-Delgado, "The Attitude Control Problem," *IEEE Trans. Auto. Contr.*, Vol. 36, No. 10, October 1991.
- [12] Widrow, B. and S.D. Stearns, *Adaptive Signal Processing*, Prentice-Hall, Englewood Cliffs, N. J., 1985.
- [13] Nering, E. D., *Linear Algebra and Matrix Theory*, Wiley, New York, 1963.

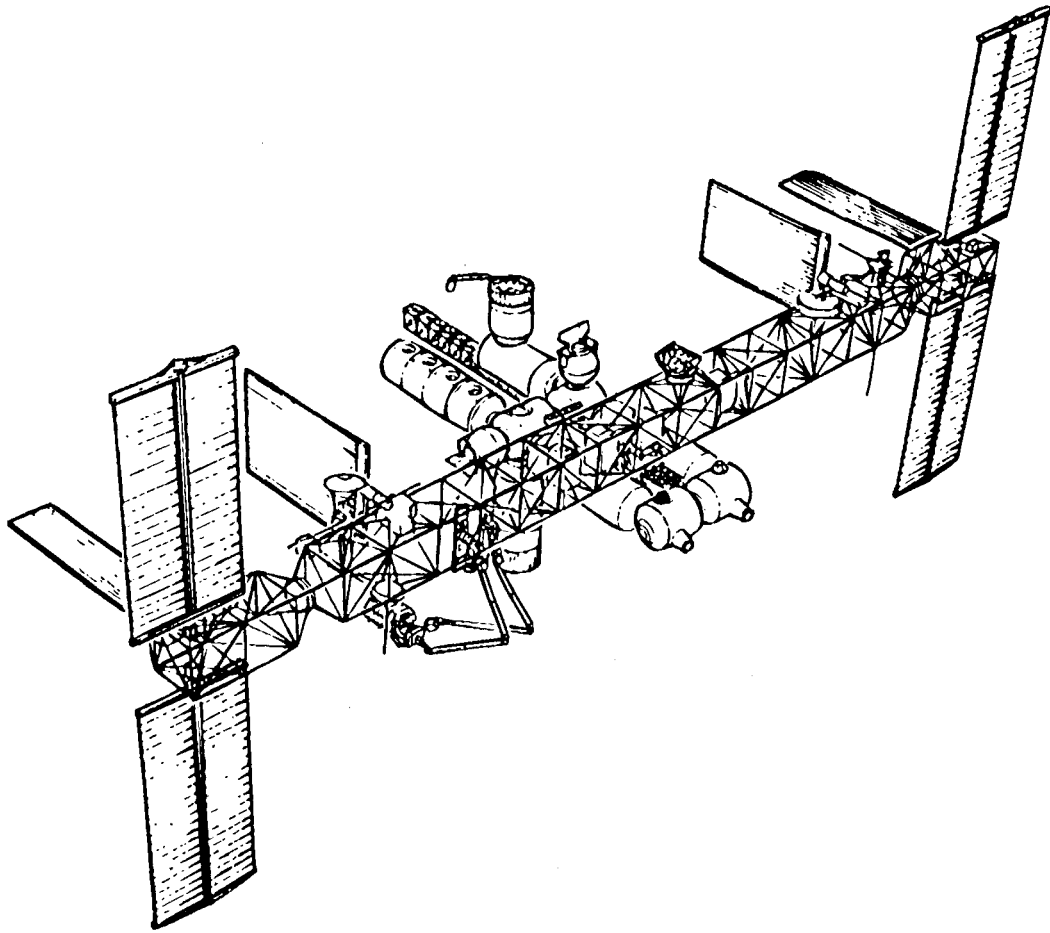


Figure 1: 'Phase 1' Configuration of the SSI'

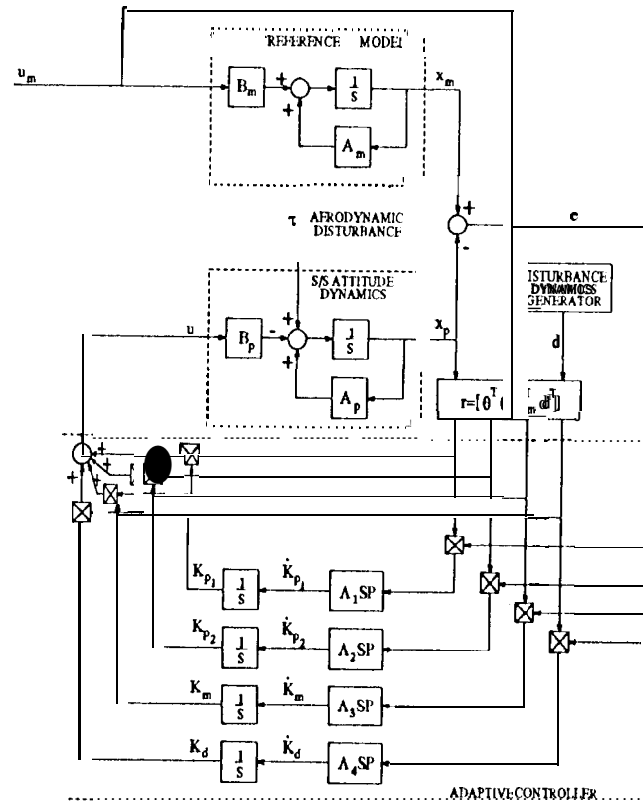


Figure 2: Adaptive Attitude Control System

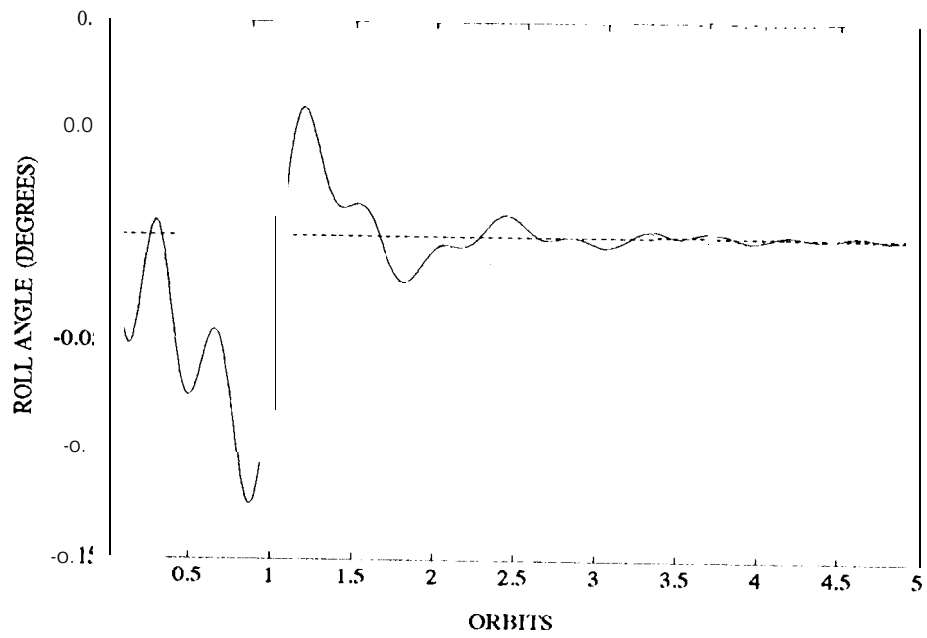


Figure 3: Case 1- Roll Angle Time Response

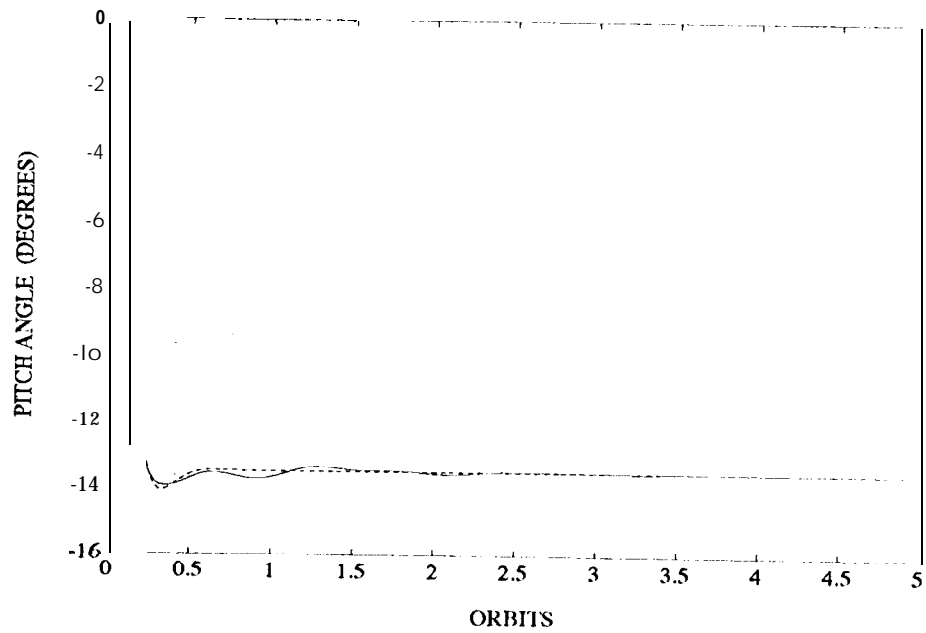


Figure 4: Case 1- Pitch Angle Time Response

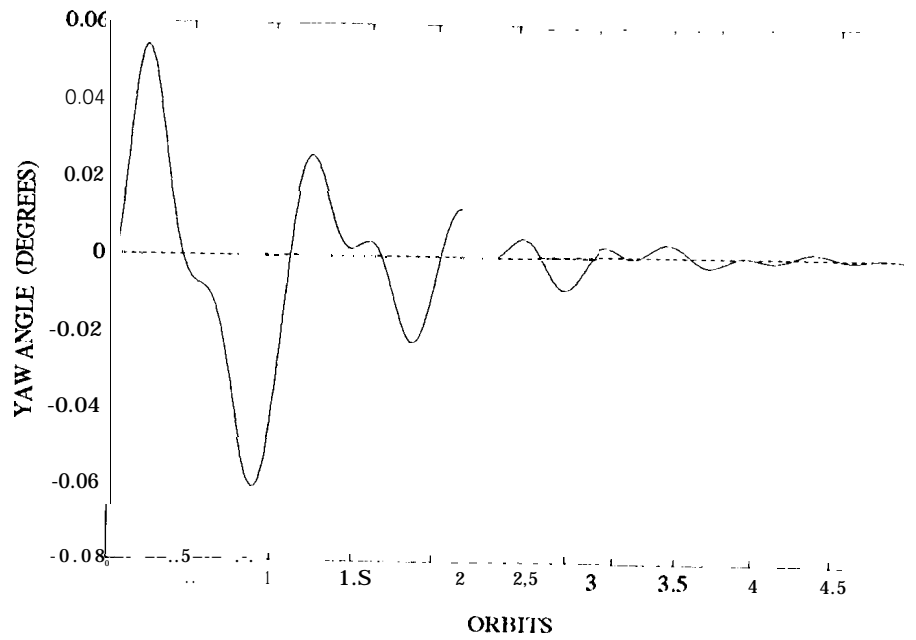


Figure 5: Case 1- Yaw Angle Time Response

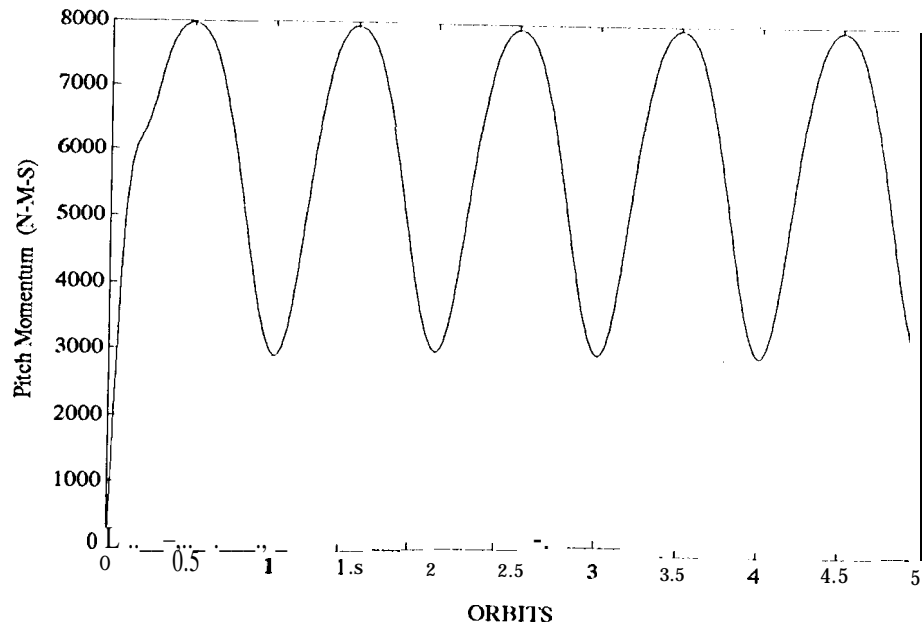


Figure 6: Case 1 - Pitch Angular Momentum

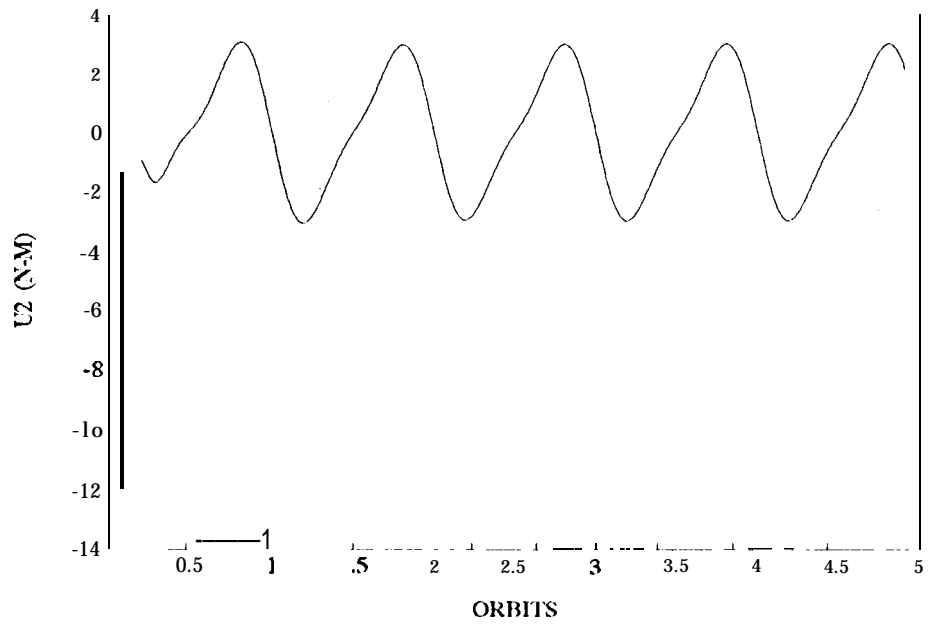


Figure 7: Case 1- Pitch Control Torque

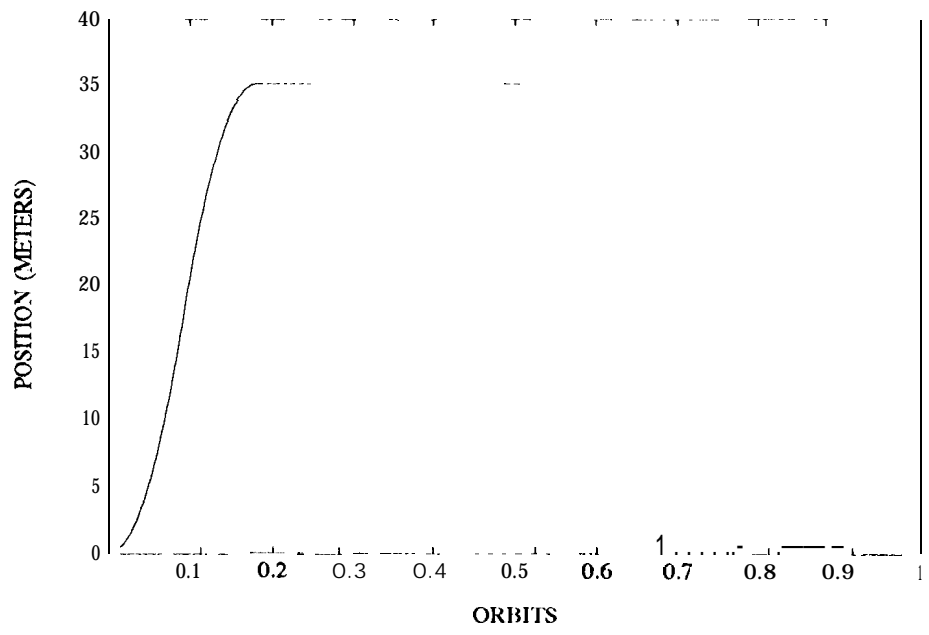


Figure 8: Case II - Payload Position Profile



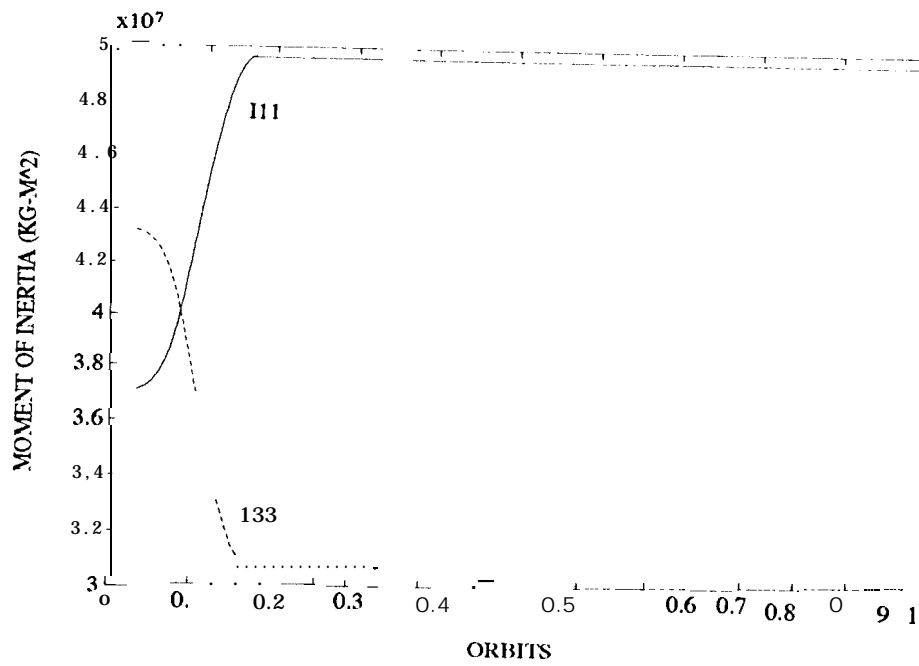


Figure 9: Case 11- Change in Moment of Inertia

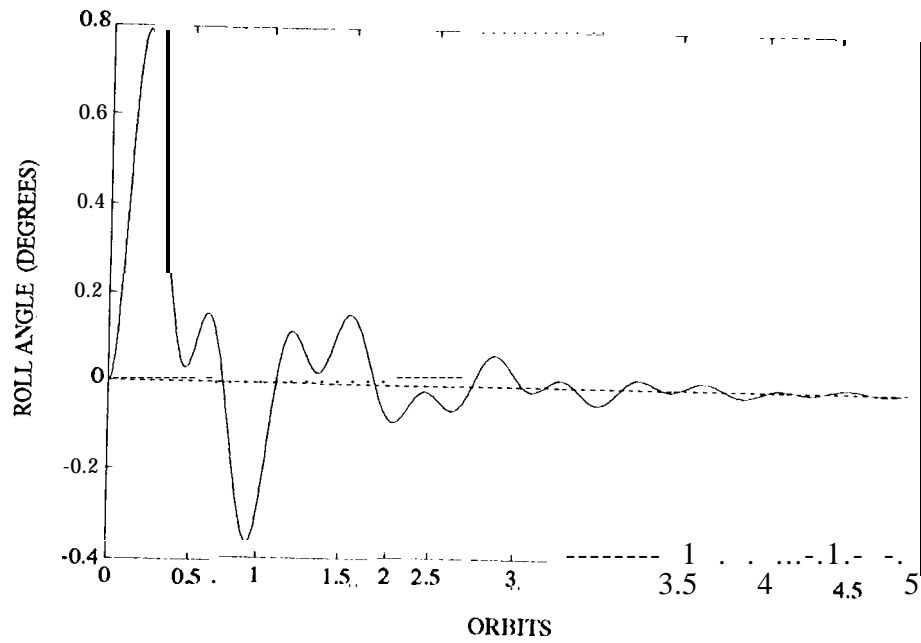


Figure 10: Case II - Roll Angle Time Response

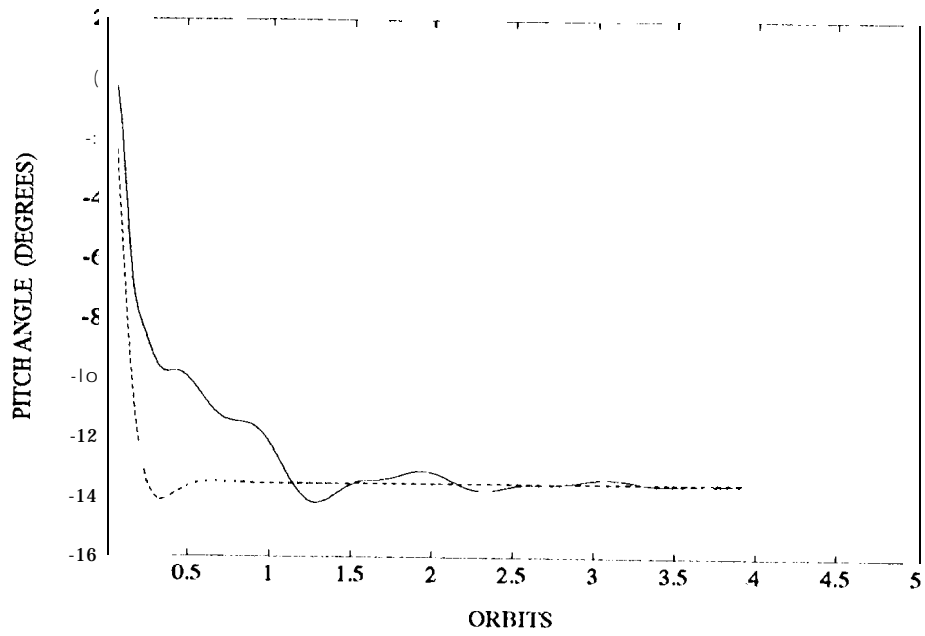


Figure 11: Case II - Pitch Angle Time Response

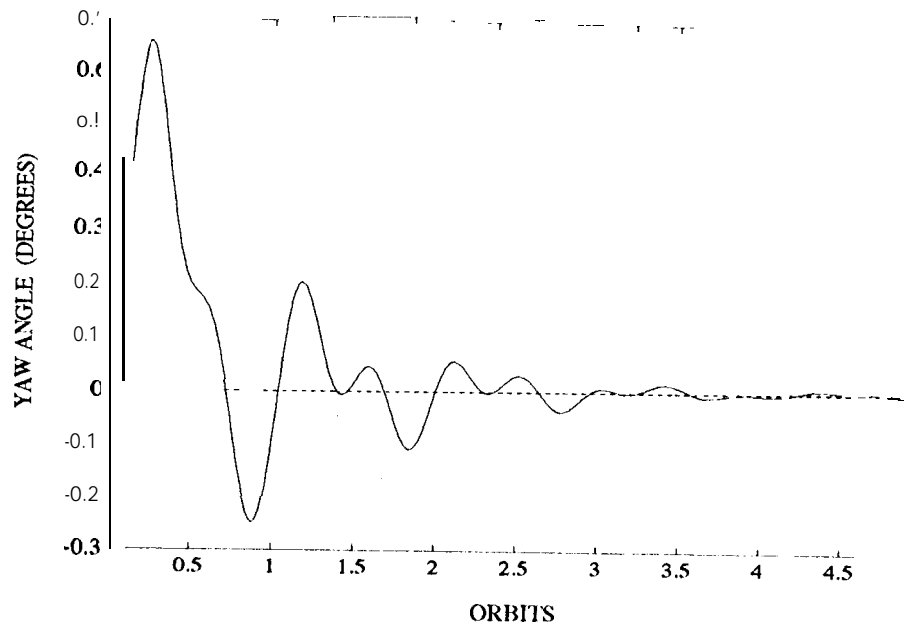


Figure 12: asc II - Yaw Angle Time Response

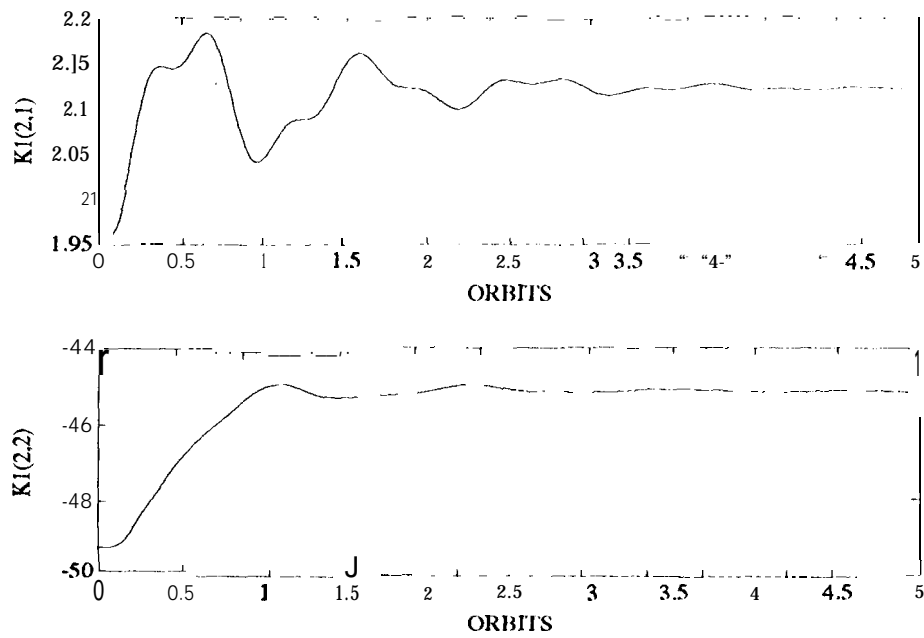


Figure 13: Case 11- Adaptation of  $K_1(2,1)$  and  $K_1(2,2)$

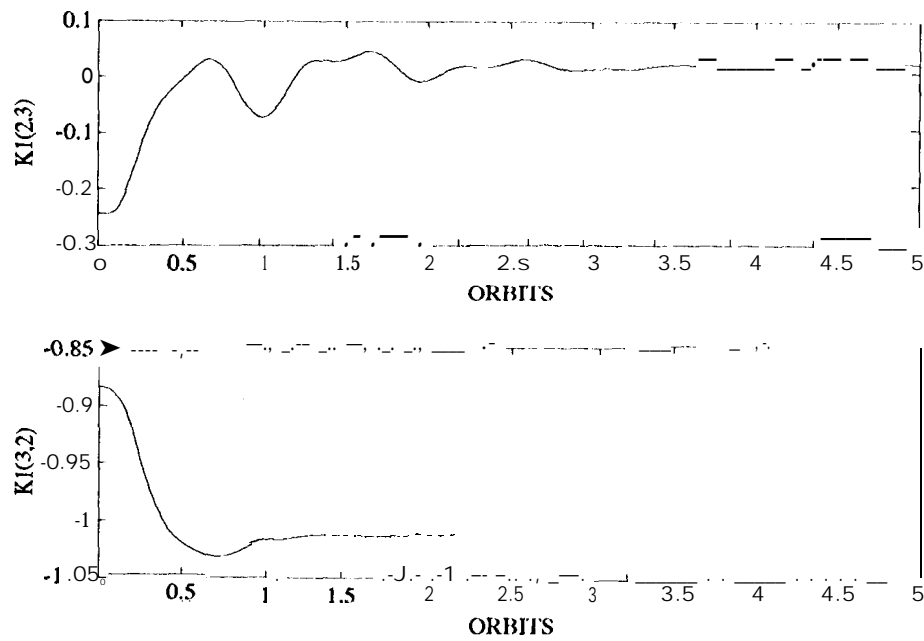


Figure 14: Case 11- Adaptation of  $K_1(2,3)$  and  $K_1(3,2)$

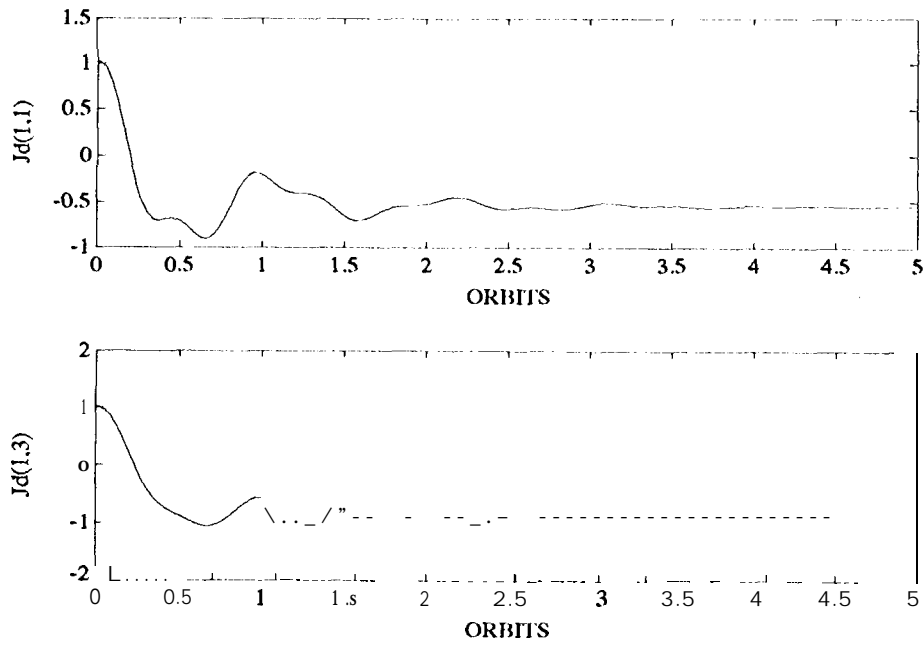


Figure 15: Case 11- Adaptation of  $J_d(1, 1)$  and  $J_d(1, 3)$

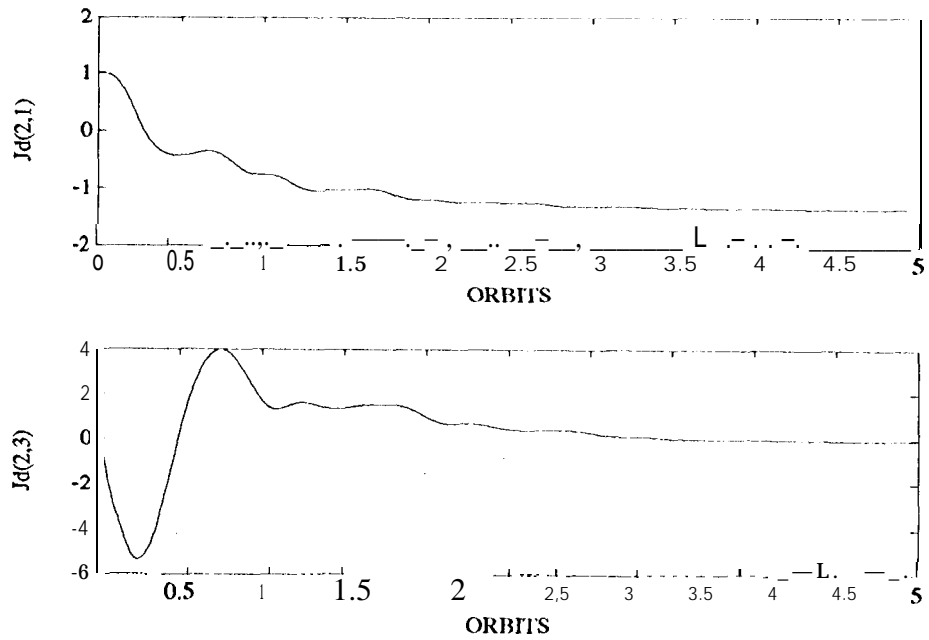


Figure 16: Case II - Adaptation of  $J_d(2, 1)$  and  $J_d(2, 3)$